



Interactive Properties of Alkaloids from *Datura stramonium*, *Moringa oleifera*, and *Carica papaya* with Human Receptor Proteins of Psychoactive Compounds from *Cannabis sativa* and *Nicotiana tabacum*

Habeeb A. Bankole¹, Rahmon I. Kanmodi^{1,2}, Mutiu I. Kazeem¹, Adedoja D. Wusu¹, Azeez A. Fatai¹, Regina T. Oddiri¹, Aaron Boakye³, Abdul-Quddus K. Oyedele⁴

¹ Department of Biochemistry, Faculty of Science, Lagos State University, Lagos, Nigeria

² Department of Oncological Sciences, University of Utah, Salt Lake City, Utah, United States

³ Department of Biochemistry, University of Utah, Salt Lake City, Utah, United States

⁴ Department of Chemistry, University of New Haven, Connecticut, United States

ARTICLE INFO

Article history:

Received : 22 February 2024

Revised : 15 March 2024

Accepted : 08 July 2024

Published online 01 August 2024

Copyright: © 2024 Bankole *et al.* This is an open-access article distributed under the terms of the [Creative Commons Attribution License](https://creativecommons.org/licenses/by/4.0/), which permits unrestricted use, distribution, and reproduction in any medium, provided the original author and source are credited.

ABSTRACT

Datura stramonium, *Moringa oleifera* and *Carica papaya* are common plants in Nigeria that have been reported to possess some psychoactive effects. However, the interactions of their alkaloids with the molecular targets of common psychoactive compounds are not well established. This study assessed the interactive potentials of alkaloids from these plants with $\alpha 4\beta 2$ nicotinic acetylcholine receptor ($\alpha 4\beta 2$ nAChR) of nicotine from *Nicotiana tabacum* and the cannabinoid receptor 1 (CB1) of delta-9-tetrahydrocannabinol (THC) from *Cannabis sativa*. Protein structures were retrieved from Protein Data Bank while PubChem was used to obtain ligand structures. Molecular docking using UCSF Chimera determined the binding affinity of protein-ligand complexes, followed by molecular dynamics simulations to evaluate root mean square deviation and radius of gyration. ADMET analysis was performed using SwissADME and ProTox-II. Notably, apotropane, hyoscyamine, and 3 $\alpha, 6\alpha$ -ditigloyloxytropine from *D. stramonium* exhibited stronger $\alpha 4\beta 2$ nAChR binding effects, compared to nicotine, and had CB1 binding affinities similar to THC. Among these high-affinity binding compounds, apotropane maintained the most stable and compact structural conformation, relative to nicotine and THC. ADMET analysis indicated propitious physicochemical and drug-like properties for all plant-based alkaloids except N, α -L-rhamnopyranosyl vincosamide from *M. oleifera* and apotropane, which were predicted to be carcinogenic. Additionally, over 50% of the plant-based alkaloids assessed are blood-brain barrier permeant, implying their propensity to mediate CNS effects. It is pertinent to regulate the use of these plants, particularly in tropical regions like Nigeria, where they are widely cultivated, consumed, and likely explored for recreational purposes based on their psychoactive effects.

Keywords: Binding affinity, Cannabinoid receptor 1, Nicotinic acetylcholine receptor, Pharmacokinetics, Plant-based alkaloids, and Psychostimulants.

Introduction

Using plants for non-medical purposes has significant public health consequences.^{1, 2} Plants belonging to this category include those used for recreational purposes, such as *Cannabis sativa* (cannabis) and *Nicotiana tabacum* (tobacco), producing mental sensations for users.^{3, 4} The most common class of bioactive compounds associated with the psychostimulatory effects of plants are alkaloids.^{5,6} Examples are the well-known nicotine and delta-9-tetrahydrocannabinol (THC), which are found in tobacco and cannabis, respectively.⁵⁻⁷ THC exerts its psychoactive effects by binding to cannabinoid receptor 1 (CB1) which has a widespread distribution in the brain,⁸ whereas nicotine interacts with neuronal alpha 4 beta 2 nicotinic acetylcholine receptor ($\alpha 4\beta 2$ nAChR).⁹

*Corresponding author. Email: rahmonilesanmi@gmail.com

Tel: +2348165549358

Citation: Bankole HA, Kanmodi RI, Kazeem MI, Wusu AD, Fatai AA, Oddiri RT, Boakye A, Oyedele AK. Interactive Properties of Alkaloids from *Datura stramonium*, *Moringa oleifera*, and *Carica papaya* with Human Receptor Proteins of Psychoactive Compounds from *Cannabis sativa* and *Nicotiana tabacum*. Trop J Nat Prod Res. 2024; 8(7):7880-7890 <https://doi.org/10.26538/tjnpr/v8i7.35>

Official Journal of Natural Product Research Group, Faculty of Pharmacy, University of Benin, Benin City, Nigeria

These interactions have been implicated in many of the adverse effects of tobacco and cannabis consumption as social stimulants, ranging from physical (respiratory, cardiovascular, stomatological and endocrine) to psychological (cognitive impairment, psychosis, anxiety and affective disorders, withdrawal symptoms, and substance dependence (DSM-5; ICD-10)),¹⁰⁻¹³ calling for their controlled use. *Datura stramonium*, *Moringa oleifera* and *Carica papaya* are plants common in Nigeria that are growing in recreational relevance due to their psychoactive effects.³ The reported mechanisms of action of the psychoactive properties of these common Nigerian plants majorly focus on their neuroactive and neurotoxicity properties.³ However, there are no reports on the binding interactions of psychoactive alkaloids derived from these plants with well-known neuronal targets such as CB1 and nAChR. Gaining knowledge of these binding interactions could provide an insight into other probable mode of action of the psychoactive effect experienced with the recreational use of these plants and justifiable reasons for government legislation of use of these plants.

Control of recreational plants and their products varies from one jurisdiction to the other; with some countries such as Nigeria adopting more stringent control measures and enforcing legislatures to prevent and criminalize the use of cannabis for medicinal and recreational purposes.¹⁴ Other control measures in Nigeria enforced by the National Drug and Law Enforcement Agency (NDLEA) target the

cultivation, possession, trafficking/distribution and sale of cannabis. This cannabis regulation by NDLEA includes penalties of up to 6 months in prison or fines for violators, and court-ordered treatment options for minors.¹⁴⁻¹⁶ Current Nigerian tobacco control laws, on the other hand, are consistent with World Health Organization (W.H.O) policies to reduce its harmful use, such as prohibitions on tobacco marketing, advertising, and sponsorship, smoking bans at indoor workplaces and public spaces, and public campaigns highlighting the dangers of tobacco consumption and secondhand inhalation.¹⁷

However, the proliferation in the recreational use of some (medicinal) plants makes their control difficult. This is attributed to several factors, including the ease of synthesizing new products from parent compounds,¹⁸ legalization of their use for non-medical/medical purposes in some countries,¹⁴ and deliberate attempts by producers to circumvent regulatory policies, especially in low- and middle-income countries.¹⁹ Additionally, natural products are widely believed to possess little or no deleterious side effects, and some plants that are not well classified as possessing psychoactive properties but serve as food sources may not receive as many regulatory measures as their counterparts with well-known psychostimulatory effects.³ Another serious concern is that plant-derived alkaloids that are used for recreational purposes could exert psychoactive effect by interacting with known receptors of natural psychoactive compounds, just like synthetic cannabinoids, cathinones, and opioids, amongst others, serving as sources of new psychoactive substances (NPS), which are now highly in use indiscriminately with no legal restriction.¹⁴ Plant-based NPS are mainly alkaloids that provide sensation and different mental states to the user when consumed.¹⁵ Identification and studies of the NPS are majorly focused on Europe, America, and Asia excluding Africa. The European Monitoring Centre for Drugs and Drug Addiction (EMCDDA) reported a spike in the use of NPS in 2019, however, there is a dearth of reports on the use and sources of NPS of African origin.¹⁶ Nonetheless, the use of NPS is also growing in numbers in Nigeria based on social-cultural belief, availability, and accessibility, mainly because most of them are plant-based and are sourced locally and freely.¹⁷

The study aims to determine the pharmacokinetics and toxicity properties of alkaloids obtained from *D. stramonium*, *M. oleifera*, and *C. papaya*, and assess their binding interactions with CB1 and $\alpha 4\beta 2$ nAChR. Notably, it is the first to analyze the interactions of these psychoactive alkaloids with these well-known targets of THC and nicotine. By employing molecular docking, molecular dynamics (MD) simulation, and *in silico* ADMET analysis, this research addresses the limitations of traditional biochemical assays, which are often time-consuming and costly.^{20, 21} These computational approaches provide precise predictions of ligand-receptor interactions and stability,²² as well as reveal the pharmacokinetics and toxicity profiles of the compounds^{23, 24}, offering a robust framework for future research and regulatory policies.

Methods

Identification and preparation of CB1 and $\alpha 4\beta 2$ nAChR proteins

CB1 and $\alpha 4\beta 2$ nAChR were downloaded from Protein Data Bank (PDB).²⁵ The proteins, CB1 and $\alpha 4\beta 2$ nAChR, with PDB IDs 5U09 and 5KXI, respectively, were prepared by removing hetatoms, and water molecules, followed by the addition of polar hydrogens and charges using Biovia Discovery Studio 4.5 software (<https://discover.3ds.com/discovery-studio-visualizer-download>).²⁶ Using the integrated Antechamber and AMBER ff14SB in UCSF Chimera v.1.17.3, Gasteiger charges were computed, and the energy of the protein backbone was minimized.²⁷

Identification and preparation of compounds for docking

Alkaloids from *Datura stramonium* (apoptropine (CID: 12306866), 3a,6a-ditigloyloxytropine (CID: 129856412), aposcopolamine (CID: 3083622), hyoscyamine (CID: 154417), scopolamine (CID: 3000322), tigloidin (CID: 12444363)); *Moringa oleifera* (N-(4-hydroxyphenyl)acetamide (CID: 1983), N, alpha L rhamnopyranosyl vincosamide (CID: 71717770), pyrroleamarumine 4"-O- α -L-rhamnopyranoside (CID: 101794622)); and *Carica papaya* (carpaine

(CID: 442630), dehydrocarpaine 1 (CID: 131750991), dehydrocarpaine II (CID:131750992)) were retrieved from PubChem in their 3D-structured data format (SDF).²⁸ Similarly, 3D-SDF conformations of reference alkaloids including Delta 9 THC (CID: 16078) and nicotine (CID :89594), as well as synthetic psychoactive compounds ABT-594 (CID: 3075702), CB 47497 (CID: 125835), JWH-018 (CID: 10382701), RCS-4 (CID: 56841530), UB-165 (CID: 4694339), and XLR-11 (CID: 57501498), were retrieved from PubChem. Spartan '14 (Wavefunction Inc., Irvine California, USA) was used to model the ligands for docking. Using the integrated Hartree-Fork basis in Spartan '14, geometry optimization and energy minimization were performed. The compounds were saved in PDB format and prepared by adding polar hydrogen and Gasteiger charges.²⁹

Molecular docking

Site-specific docking was performed using AutoDock Vina³⁰ integrated with UCSF Chimera v.1.17.3. The docking method was validated by first extracting the co-crystallized/standard ligands (THC and nicotine) and then redocking them precisely into the active sites of their corresponding proteins, maintaining the original grid parameters (5U09-THC: x= 21.0561, y= 2.0225, z= -10.7851; and 5KXI-nicotine: x= 75.8315, y= 19.7954, z= -26.4367) and protocols throughout the process. The binding energies of the complexes were subsequently generated and recorded.

Molecular dynamics (MD) simulation

GROMACS v.2018.6 (GROningen MACHine for Chemical Simulations) MD environment was utilized to set up the simulations for the protein complexes,³¹ involving 5KXI (5KXI-nicotine, 5KXI-apoptropine, and 5KXI-hyoscyamine) and 5U09 (5U09-Delta 9 THC, 5U09-apoptropine, and 5U09-3a,6a-ditigloyloxytropine). The protein topology was computed using the TIP3P CHARMM-modified water model³² and the CHARMM36 all-atom force field.³³ Meanwhile, CGENFF web server³³ and the Avogadro software³⁴ were employed to prepare ligand topology, generating ".str" files and ".mol2" respectively, which were then manually updated to incorporate ligands using GROMACS commands. Each system was ionized and neutralized before the additional solvation step produced with the TIP3P CHARMM-modified water model. Stabilization of the system conformation was achieved by carrying out energy minimization for 100 ps using descending algorithm at the steepest level. This was followed by a two-phase equilibration: NVT equilibration from 0 to 310 K over 100 ps with a 2 fs time step using the Verlet algorithm, and NPT equilibration for 100 ps with a 2 fs time step using the Berendsen algorithm³⁵. The "trjconv" module was applied to maintain the protein in a central position and compact form, ensuring atoms remained within periodic boundary condition (PBC). Upon equilibrating the system, MD simulations were performed for 20 ns with no restraints, employing an integration time step of 2 fs while recording trajectory snapshots every 1 ps. The MD trajectories were subsequently analyzed for key metrics such as the Radius of Gyration (ROG), and Root Mean Square Deviation (RMSD), while the Qtgrace software (<https://sourceforge.net/projects/qtgrace/>) was employed to plot the graph spectrum.³⁶

Analysis of ligand-protein interactions

The 2D and 3D images of protein-ligand interactions were captured using Biovia Discovery Studio Visualizer 4.5.²⁶

Absorption, Distribution, Metabolism, Excretion and Toxicity (ADMET) Analysis

The compounds' canonical smiles were obtained from PubChem using their CIDs and then submitted to the SwissADME server; a comprehensive, user-friendly, and free tool for evaluating chemical ADME properties.³⁷ ProTox-II was used to perform toxicity testing for Ames mutagenicity and carcinogenicity.³⁸

Results and Discussion

Binding affinity predictions are crucial in determining how chemical compounds interact with their targets to elicit biological effects.^{39,40} *D. stramonium* alkaloids - apotropine and hyoscyamine - ranked higher

in binding affinity with $\alpha 4\beta 2$ nAChR than other plant alkaloids, the reference nicotine, and synthetic psychoactive compounds (Table 1).

Table 1: Binding energies in Kcal/mol of the interactions of psychoactive compounds with neuronal protein targets.

S/N	Psychoactive Compounds	Cannabinoid Receptor I (CB1)	Human Alpha 4 Beta 2 Nicotinic Acetylcholine Receptor ($\alpha 4\beta 2$ nAChR)
Alkaloids from well-known psychoactive plants			
<i>Cannabis sativa</i>			
<i>Nicotiana tabacum</i>			
1	Delta-9-tetrahydrocannabinol	-9.4	-
2	Nicotine	-	-5.3
<i>Carica papaya</i>-derived alkaloids			
3	Carpaine	-5.9	-4.8
4	Dehydrocarpaine I	-6.4	-4.6
5	Dehydrocarpaine II	-6.8	-4.9
<i>Moringa oleifera</i>-derived Alkaloids			
6	N, α -L-rhamnopyranosyl vincosamide	-2.9	-6.0
7	Pyrolemarumine 4"- <i>O</i> - α -L-rhamnopyranoside	-8.5	-6.6
8	4'hydroxyphenylethanamide	-6.1	-6.5
<i>Datura stramonium</i>-derived alkaloids			
9	Scopolamine	-8.1	-7.2
10	Tigloidin	-7.6	-6.6
11	Aposcopolamine	-8.7	-7.4
12	Apoatropine	-8.9	-7.9
13	3 α ,6 α -ditigloyloxytropene	-8.8	-7.0
14	Hyoscyamine	-8.4	-7.8
Synthetic psychoactive compounds			
15	⁺ CB 47497: 2-[(1 <i>r</i> ,3 <i>s</i>)-3-Hydroxycyclohexyl]-5-(2-methyloctan-2-yl) phenol	-9.0	-6.4
16	⁺ JWH-018: 1-Pentyl-3-(1-naphthoyl) indole	-10.1	-6.1
17	⁺ RCS-4: 1-Pentyl-3-(4-methoxybenzoyl) indole	-9.2	-6.7
18	⁺ XLR-11: (1-(5-Fluoropentyl)-1 <i>H</i> -indol-3-yl) (2,2,3,3-tetramethylcyclopropyl) methanone	-8.7	-6.2
19	*UB-165: 5-(6-Chloro-3-pyridinyl)-9-azabicyclo [4.2.1] non-4-ene	-8.2	-6.1
20	*ABT-594: 5-(2-azetidylmethoxy)-2-chloropyridine	-6.1	-6.0

⁺ Synthetic cannabinoid receptor agonists

* Synthetic human alpha 4 beta 2 nicotinic acetylcholine receptor agonists

THC, however, was the best CB1-binding natural alkaloid, with *D. stramonium* compounds, apoatropine and 3a,6a-ditigloyloxytropine, emerging as second and third best, respectively. Hyoscyamine and atropine have been implicated in the neuromodulatory effects of *D. stramonium*.^{41, 42} These alkaloids act as competitive antagonists at muscarinic acetylcholine receptors to stimulate or depress the CNS system.³ The higher binding affinities exhibited by these alkaloids with $\alpha 4\beta 2$ nAChR and CB1 suggest that they will readily bind the two receptors and may inhibit or elicit similar effects as their natural substrates. This is important, especially considering that low binding energy compounds interact with their targets with greater specificity, resulting in significant biological effects.⁴³ This also implies that these alkaloids may be associated with *D. stramonium*'s psychoactive effects. It is, however, important to further investigate the structural and molecular bases of these compounds' high binding interactions with $\alpha 4\beta 2$ nAChR and CB1 using *in vitro* and *in vivo* studies to delineate their psychostimulatory effects.

Aside from the *D. stramonium* alkaloids, pyrrolemarumine 4''-O- α -L-rhamnopyranoside derived from *M. oleifera* displayed high CB1 and $\alpha 4\beta 2$ nAChR binding affinities, while *C. papaya* compounds – carpaine, dehydrocarpaine I and dehydrocarpaine II – exhibited moderate CB1 binding affinities. This suggests that the reported psychoactive effects of *M. oleifera* and *C. papaya* may be due to the presence of these alkaloid reservoirs. According to numerous studies, the main bioactive constituents in *C. papaya* are carpaine, and its structural analogs dehydrocarpaine I and dehydrocarpaine II.⁴⁴⁻⁴⁷ Previous reports have indicated that carpaine is one of the main bioactive constituents in papaya that has been linked to its central nervous system (CNS) stimulatory effects.^{3,48} Carpaine, dehydrocarpaine I and dehydrocarpaine II, are present in varying quantities in papaya varieties: fruit bearing (pistillate or female), non-fruit bearing (staminate or male), and bisexual.^{45-47, 49, 50} The highest concentration of carpaine is found in mature papaya leaves, followed by the fruit pulp, fruit peel and seeds.⁵¹ The presence of carpaine, dehydrocarpaine I and dehydrocarpaine II in papaya fruits, leaves and seeds may increase the likelihood of psychotropic effects in people who consume them for food, medicine, or recreation. More insights about the psychoactive effects of *C. papaya* could be gained by investigating how carpaine, dehydrocarpaine I, and dehydrocarpaine II concentrations vary across different papaya species, sex types, and maturation periods. Metabolic profiling of papaya fruit has revealed that the levels of dehydrocarpaine I and dehydrocarpaine II decrease as papaya fruit ripens.⁵² More studies of this nature will be invaluable for regulatory authorities to isolate the effects of biological and ecological factors on the psychostimulatory properties of papaya. It will also provide insights into the developmental processes of many recreational plants that are more likely to impact their psychoactive properties.

The interactions leading to the high binding affinities observed for apoatropine and 3a,6a-ditigloyloxytropine with CB1, and apoatropine and hyoscyamine with $\alpha 4\beta 2$ nAChR, are illustrated in figures 1 and 2, respectively. In our study, TYR 197 was a common interacting residue in all three high-affinity $\alpha 4\beta 2$ nAChR -ligand complexes. Specifically, it formed Pi-Pi T-shaped bonds in the $\alpha 4\beta 2$ nAChR-apoatropine and $\alpha 4\beta 2$ nAChR-hyoscyamine complexes and van der Waals interactions in the $\alpha 4\beta 2$ nAChR-nicotine complex. According to a previous study,⁵³ amino acids between 181–200 of the nAChR $\alpha 1$ subunit are essential for nicotine binding. High-resolution structural studies involving Xray and cryogenic electron microscopy (Cryo-EM) further revealed that interactions from Tyr-197 and Tyr-204, along with neighboring cysteine residues, tightly pack nicotine within the binding pocket of $\alpha 4\beta 2$ nAChR.⁵⁴ Thus, TYR 197, as well as CYS 192, CYS 193 residues present in the interactions of both apoatropine and hyoscyamine to $\alpha 4\beta 2$ nAChR may be key contributors to their high-affinity binding over nicotine, as depicted in Table 1. The presence of Pi-Pi T shaped interaction involving TRP 149 in the $\alpha 4\beta 2$ nAChR – apoatropine and $\alpha 4\beta 2$ nAChR – hyoscyamine complexes is especially significant and may also contribute to their high affinity binding with $\alpha 4\beta 2$ nAChR. A previous study revealed that high-affinity endogenous

(acetylcholine) and exogenous (nicotine) $\alpha 4\beta 2$ nAChR compounds form a strong Pi-cation interaction with TRP, chain B-residue 149 of $\alpha 4\beta 2$ nAChR.⁵⁵ Moreover, both apoatropine and hyoscyamine exhibit multiple types of strong interactions, such as Pi-alkyl and Pi-Pi alkyl with CYS 192, CYS 193, and LEU 484, as well as attractive charge interactions and Pi-sigma/Pi-cation interactions with GLU 195 and PHE 482. These interactions could contribute significantly to their binding strength and stability within the receptor's binding pocket. In contrast, nicotine predominantly relies on van der Waals interactions involving residues like TRP 57, CYS 199, PHE 119, VAL 111, and THR 157. The

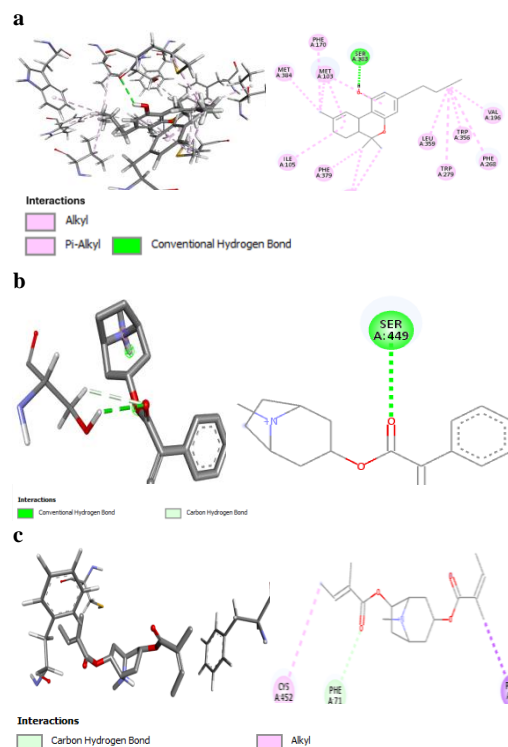


Figure 1: 3D and 2D protein-ligand interactions of CB1 and THC (a), CB1 and apoatropine (b), and CB1 and 3a,6a-ditigloyloxytropine (c)

significance of identifying new interactions that may contribute to selective and potent binding cannot be overemphasized, particularly for determining agonist/antagonist of multisubunit protein such as $\alpha 4\beta 2$ nAChR with complex structural motifs.⁵⁴ Interestingly, apoatropine and 3a,6a-ditigloyloxytropine did not share any common interactions with the reference compound, THC, despite binding to the same site occupied by THC on CB1 and exhibiting comparable CB1 binding affinities to THC. This discrepancy may be attributed to the distinct structural motifs present in THC compared to these two compounds derived from *D. stramonium*. The site-specific docking approach employed in our study is instrumental in revealing ligand interactions within target protein binding pockets, identifying potential new interactors, and predicting ligands with high-binding affinities.⁵⁶ However, it lacks the ability to independently discern interactions critical for agonist binding efficacy from incidental ones, particularly crucial when compared with psychostimulants.⁵⁷ Additionally, site-specific docking may not fully account for conformational changes in proteins and ligands, especially in flexible regions or upon binding, potentially leading to inaccuracies in binding predictions.^{39, 58} To address these limitations and enhance reliability, we complemented our docking approach with MD simulations. MD simulations enable us to explore the dynamic behavior, flexibility, and stability of complexes over time,^{39, 40} offering a more comprehensive understanding within a biological context and lowering false positive outcomes.⁴⁰ Thus, we conducted a 20 ns MD simulation on four high-affinity protein-ligand complexes from test plants ($\alpha 4\beta 2$ nAChR-

apoptropine, $\alpha 4\beta 2$ nAChR-hyoscyamine, CB1-apoptropine, and CB1-3a,6a-ditigloyloxytropine) to compare their dynamics with the standard compounds, THC and nicotine, using RMSD and ROG metrics. RMSD provides a detailed view of the stability and conformational changes of the compounds over the entire simulation period,³⁶ while ROG reveals the overall compactness and folding of compounds during simulation events.³⁶

Our MD simulations revealed average RMSD values of 0.26 nm and 0.61 nm for the standards, THC and nicotine, respectively, indicating that they maintain their structure very well and show high stability in binding their tar. Furthermore, the $\alpha 4\beta 2$ nAChR-bound compounds –

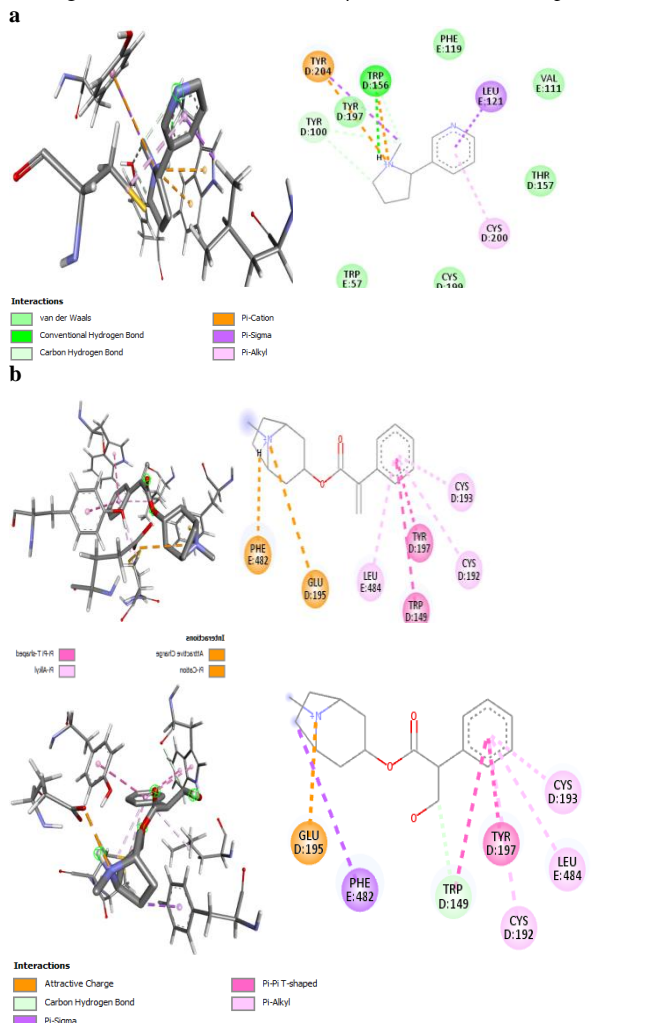


Figure 2: 3D and 2D protein-ligand interactions of $\alpha 4\beta 2$ nAChR and nicotine (a), $\alpha 4\beta 2$ nAChR and apoptropine (b), and $\alpha 4\beta 2$ nAChR and hyoscyamine (c)

apoptropine and hyoscyamine - exhibit higher RMSD values (Fig. 4), suggesting they undergo more significant conformational changes and are less stable than their CB1 interacting counterparts. The RMSD for hyoscyamine shows a similar trend to apoptropine, with an initial rise and then a stabilization phase at a higher RMSD value. The high average RMSD of 0.93 nm indicates considerable structural fluctuations, suggesting that hyoscyamine is the least stable among the $\alpha 4\beta 2$ nAChR compounds. The CB1-bound compounds, apoptropine and 3a,6a-ditigloyloxytropine, with their lower RMSD values of 0.27 and 0.29 nm, respectively, demonstrate better structural stability throughout the simulation (Fig. 3). The ROG graphs show that the CB1 compounds, with their higher ROG values, have more consistent extended structures while the $\alpha 4\beta 2$ nAChR compounds have more compact and variable conformations (Fig. 5 and 6). Like THC, apoptropine maintains a high and relatively stable ROG value,

indicating an extended structure throughout the simulation. 3a,6a-ditigloyloxytropine has the highest average ROG value (3.06 nm), indicating it adopts the most extended conformation among the CB1 compounds. The ROG graph shows moderate fluctuations, suggesting variability in its extended structure. On the other hand, the ROG graph for nicotine shows moderate fluctuations around the average value of 2.16 nm, indicating that the compound maintains a relatively compact structure but experiences some variations in its folding. Apoptropine has the lowest average ROG (2.11 nm) among the $\alpha 4\beta 2$ nAChR compounds, suggesting it maintains the most compact structure. The ROG graph shows minimal fluctuations, indicating consistent

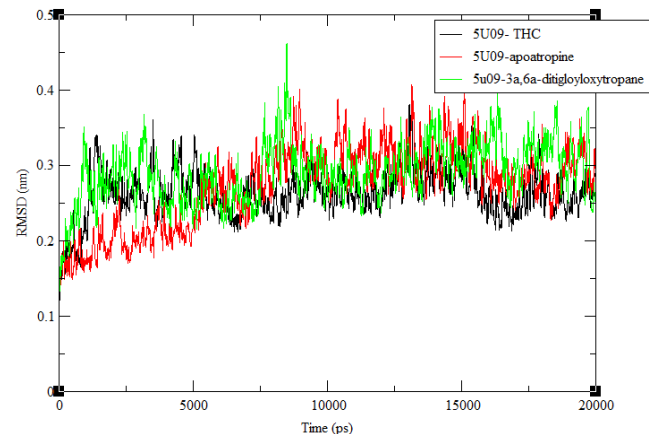


Figure 3. RMSD spectrums of the two high-affinity compounds (apoptropine, and 3a,6a-ditigloyloxytropine) and the standard, THC, in CB1 (5U09) pocket.

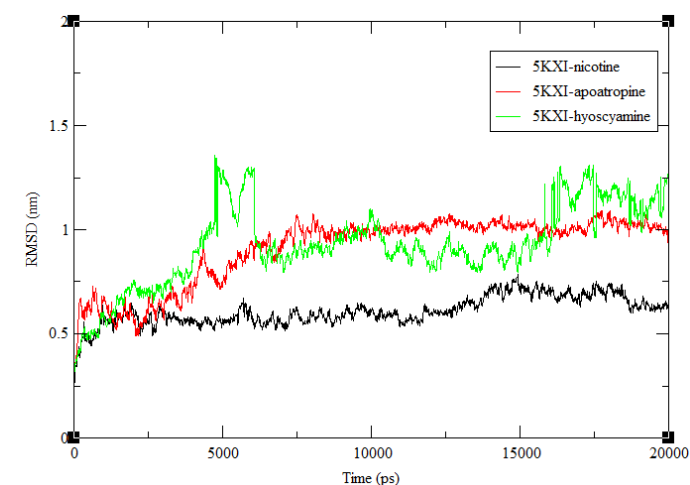


Figure 4. RMSD spectrums of the two high affinity compounds (apoptropine, and hyoscyamine) and the standard, nicotine, in $\alpha 4\beta 2$ nAChR (5KXI) pocket.

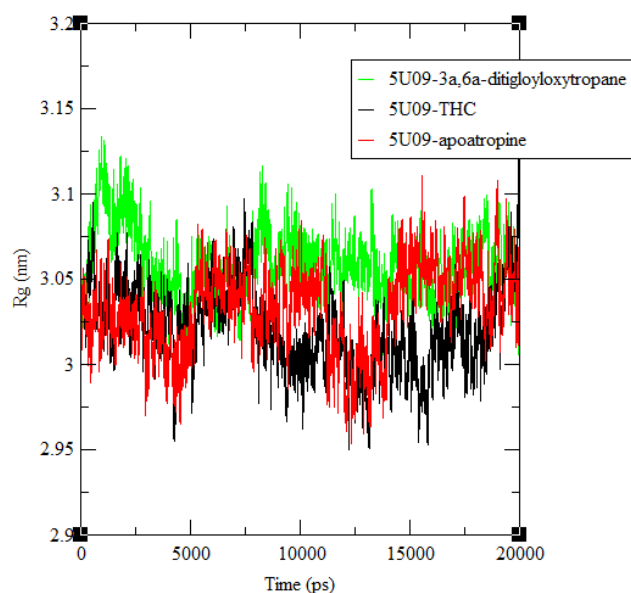


Figure 5: ROG spectra of the two high-affinity compounds (apoatropine, and 3a,6a-ditigloyloxytropene) and the standard, THC, in CB1 (5U09) pocket.

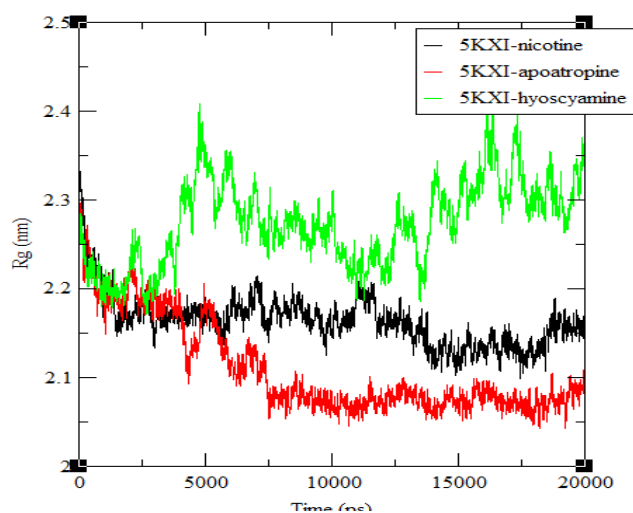


Figure 6: ROG spectra of the two high affinity compounds (apoatropine, and hyoscyamine) and the standard, nicotine, in $\alpha 4\beta 2$ nAChR (5KXI) pocket.

compactness. The ROG graph for hyoscyamine indicates more significant fluctuation, reflecting a less compact and more variable structure throughout the simulation. This is consistent with its higher average ROG value of 2.27 nm.

ADMET analysis is crucial in assessing the safety and pharmacokinetic properties of chemical compounds.⁵⁹ It was discovered from this study that all test alkaloids, except N,-L-rhamnopyranosyl vincosamide, met the Lipinski cut-off (Tables 2a and 2b); demonstrating their propensity for adequate absorption and permeability from an oral bioavailability perspective.⁶⁰ The Lipinski rule predicts that compounds with zero or at most one violation will have high oral bioavailability.^{61, 62} Specifically, N,-L-rhamnopyranosyl

vincosamide exceeded the limits for molecular weight (>500 Daltons), hydrogen bond donors (>5), and hydrogen bond acceptors (>10) (Table 2a). For a chemical compound with high oral bioavailability, a small dose is required to achieve the desired pharmacological effect.^{63, 64} According to the findings from this study, many of the alkaloids including THC, nicotine, apoatropine, 3a,6a-ditigloyloxytropene, aposcopolamine, hyoscyamine, tigloidin, and N-(4-hydroxyphenyl) acetamide have high BBB permeability. Compounds with high BBB permeability can interact with CNS receptors and mediate neuronal effects. The alkaloids' high BBB permeability may contribute to the psychoactive effects of the plants where they are present. N,-L-rhamnopyranosyl vincosamide, dehydrocarpaine I and dehydrocarpaine II were predicted to be P-glycoprotein substrates amongst the plant alkaloids. Substrates of P-glycoprotein transporter exhibit unfavorable pharmacokinetics, hindering their absorption and distribution in various organs.^{65,66} Therefore, many of the test alkaloids that are non-P-glycoprotein substrates have greater possibilities for absorption and permeability through body tissues and cells. This is particularly concerning for compounds that are used for recreational purposes, as they are likely abused or overdosed, leading to accumulating harmful concentrations in tissues and cells.

Based on the oral toxicity test, nicotine was predicted to fall into class I ($LD_{50} \leq 5$ mg/kg), indicating the highest risk of fatality if swallowed. Other compounds are classified as class III (50 mg/kg $< LD_{50} \leq 300$ mg/kg), class IV (300 mg/kg $< LD_{50} \leq 2000$ mg/kg), or class V (2000 mg/kg $< LD_{50} \leq 5000$ mg/kg), denoting a decreasing likelihood of causing fatality upon ingestion, respectively.⁶⁷ Toxicity testing also revealed that none of the test plant alkaloids are Ames mutagenic. It is noteworthy to mention that apoatropine and N, α -L-rhamnopyranosyl vincosamide from *D. stramonium* and *M. oleifera*, respectively, are predicted to be carcinogenic (Table 2a), implying that these plant alkaloids should be monitored very strictly by food and drug regulatory agencies, especially in areas where they are considered as mainstream recreational products.

Table 2a: ADMET Properties of Alkaloids from *Cannabis sativa*, *Nicotiana tabacum*, *Carica papaya*, *Moringa oleifera*, and *Datura stramonium*

Properties	Delta-9-tetrahydrocannabinol	Nicotine	Carpaine	Dehydrocarpaine I	Dehydrocarpaine II	N, α -L-rhamnopyranosyl vincosamide	Pyrolemarminone 4'-O- α -L-rhamnopyranoside	4'-hydroxyphenylethylamine
MW (Daltons)	314.46	162.23	478.71	476.69	474.68	660.67	377.39	151.16
AlogP	5.74	1.14	4.64	4.83	5.07	-1.50	0.08	0.93
H-Bond Acceptor	2	2	6	6	6	13	7	2

H-Bond Donor	1	0	2	1	0	7	4	2
Rotatable Bonds	4	1	0	0	0	6	6	2
BBB Permeability	Yes	Yes	No	No	No	No	No	Yes
GI Absorption	High	High	High	High	High	Low	High	High
Oral Toxicity	Class 4	Class 1	Class 4	Class 4	Class 5	Class 4	Class 5	Class 4
LD ₅₀ (mg/kg)	482	3	500	500	3000	620	4000	338
P-glycoprotein Substrate	No	No	No	Yes	Yes	Yes	No	No
CYP1A2 Inhibitor	No	No	No	No	No	No	Yes	No
CYP2C19 Inhibitor	Yes	No						
CYP2C9 Inhibitor	Yes	No						
CYP2D6 Inhibitor	Yes	No						
CYP3A4 inhibitor	No							
Bioavailability Score	0.55	0.55	0.55	0.55	0.55	0.11	0.55	0.55
Ames toxicity	Inactive 0.77	Inactive 0.91	Inactive 0.80	Inactive 0.76	Inactive 0.75	Inactive 0.52	Inactive 0.66	Inactive 0.90
Carcinogenicity	Inactive 0.86	Inactive 0.91	Inactive 0.62	Inactive 0.59	Inactive 0.54	Active 0.51	Inactive 0.60	Inactive 0.51

MW: Molecular weight; AlogP: Octanol-water partition coefficient; BBB: Blood-Brain Barrier; GI: Gastrointestinal; CYP: Cytochrome P450

Table 2a (Continue...): ADMET Properties of Natural Psychoactive Compounds from *Nicotiana tabacum*, *Cannabis sativa*, *Moringa oleifera*, *Datura stramonium*, and *Carica papaya*

Properties	Scopolamine	Tigloidin	Aposcopolamin	Apoatropine	3 α ,6 α -dihydroxytropane	Hyoscyamine
MW (Daltons)	303.35	223.31	285.34	271.35	321.41	289.37
AlogP	1.38	2.22	2.11	2.94	2.78	2.06
H-Bond Acceptor	5	3	4	3	5	4
H-Bond Donor	1	0	0	0	0	1
Rotatable Bonds	5	3	4	4	6	5
BBB Permeability	No	Yes	Yes	Yes	Yes	Yes
GI Absorption	High	High	High	High	High	High
Oral Toxicity	Class 4	Class 4	Class 4	Class 3	Class 5	Class 4
LD ₅₀ (mg/kg)	1275	705	1500	160	2573	380
P-glycoprotein	No	No	No	No	No	No

Substrate						
CYP1A2 Inhibitor	No	No	No	No	No	No
CYP2C19 Inhibitor	No	No	No	No	No	No
CYP2C9 Inhibitor	No	No	No	No	Yes	No
CYP2D6 Inhibitor	Yes	No	Yes	Yes	No	Yes
CYP3A4 inhibitor	No	No	No	No	No	No
Bioavailability	0.55	0.55	0.55	0.55	0.55	0.55
Score						
Ames toxicity	Inactive	Inactive	Inactive	Inactive	Inactive	Inactive
	0.88	0.67	0.61	0.68	0.66	0.76
Carcinogenicity	Inactive	Inactive	Inactive	Active	Inactive	Inactive
(class three)	0.75	0.51	0.55	0.56	0.51	0.86

Table 2b: ADMET Properties of Synthetic Psychoactive Compounds

Properties	CB 47497	JWH-018	RCS-4	XLR-11	UB-165	ABT-594
MW (Daltons)	318.49	341.45	321.41	329.45	234.72	198.65
AlogP	5.18	5.32	4.39	4.96	2.68	1.59
H-Bond Acceptor	2	1	2	2	2	3
H-Bond Donor	2	0	0	0	1	1
Rotatable Bonds	7	6	7	7	1	3
BBB Permeability	Yes	No	Yes	No	Yes	Yes
GI Absorption	High	High	High	High	High	High
Oral Toxicity	Class 5	Class 4	Class 4	Class 3	Class 3	Class 4
LD ₅₀ (mg/kg)	4000	500	2000	200	200	350
P-glycoprotein	No	Yes	No	Yes	Yes	No
Substrate						
CYP1A2 Inhibitor	No	Yes	Yes	Yes	Yes	Yes
CYP2C19 Inhibitor	No	Yes	Yes	No	No	No
CYP2C9 Inhibitor	No	Yes	Yes	No	No	No
CYP2D6 Inhibitor	Yes	Yes	Yes	Yes	Yes	No
CYP3A4 inhibitor	No	Yes	Yes	Yes	No	No
Bioavailability	0.55	0.55	0.55	0.55	0.55	0.55
Ames toxicity	Inactive	Active	Active	Inactive	Inactive	Inactive
	0.88	0.61	0.59	0.56	0.64	0.53
Carcinogenicity (class	Inactive	Inactive	Inactive	Inactive	Inactive	Active

three) 0.79 0.60 0.56 0.59 0.78 0.62

Conclusion

The findings showed that alkaloids from *M. oleifera*, *C. papaya*, and especially *D. stramonium* (apoatropine, hyoscyamine and 3 β ,6 α -ditigloyloxytropine) exhibited strong binding affinity with CB1 and α 4 β 2 nAChR, relative to THC and nicotine, respectively. Furthermore, most of these plant alkaloids displayed favorable physicochemical and druglike properties, as well as high BBB permeability, suggesting a potential for CNS effects while apoatropine and *M. oleifera*-derived N, α -L-rhamnopyranosyl vincosamide were predicted to be carcinogenic. Thus, it is critical to regulate the recreational consumption of these plants, particularly in tropical regions like Nigeria, where they are widely cultivated and consumed for various purposes. The Nigerian government should also enforce legislation to limit the recreational market from exploring parent psychoactive compounds from these plants for NPS synthesis. *In vitro* and *in vivo* experiments are recommended to explicitly decipher the structural and molecular mechanisms by which these alkaloids interact with CB1 and α 4 β 2 nAChR, as well as other neuronal targets to directly link them to the psychoactive effects of *D. stramonium*, *M. oleifera*, and *C. papaya*.

Conflict of Interest

The authors declare no conflict of interest.

Authors' Declaration

The authors hereby declare that the work presented in this article is original and that any liability for claims relating to the content of this article will be borne by them.

Acknowledgements

We acknowledge the technical assistance provided by the Bioinformatics Unit of the Department of Biochemistry, Lagos State University, during this study.

References

1. Simão AY, Antunes M, Cabral E, Oliveira P, Rosendo LM, Brinca AT, Alves E, Marques H, Rosado T, Passarinha LA. An update on the implications of new psychoactive substances in public health. *Int J. Environ Res Public Health*. 2022; 19(8):4869.
2. Wolfe D, Corace K, Butler C, Rice D, Skidmore B, Patel Y, Thayaparan P, Michaud A, Hamel C, Smith A. Impacts of medical and non-medical cannabis on the health of older adults: Findings from a scoping review of the literature. *Plos one*. 2023; 18(2):e0281826.
3. Fasakin OW, Oboh G, Ademosun AO. The prevalence, mechanism of action, and toxicity of Nigerian psychoactive plants. *Comp. Clin. Path*. 2022; 31(5):853-873.
4. Jamieson CS, Misa J, Tang Y, Billingsley JM. Biosynthesis and synthetic biology of psychoactive natural products. *Chem. Soc. Rev*. 2021; 50(12):6950-7008.
5. Khalsa JH, Bunt G, Blum K, Maggirwar SB, Galanter M, Potenza MN. Cannabinoids as medicinals. *Curr. Addict. Rep*. 2022; 9(4):630-646.
6. Rehan HS, Maini J, Hungin AP. Vaping versus smoking: a quest for efficacy and safety of E-cigarette. *Curr. Drug Saf*. 2018; 13(2):92-101.
7. McDonagh MS, Morasco BJ, Wagner J, Ahmed AY, Fu R, Kansagara D, Chou R. Cannabis-based products for chronic pain: a systematic review. *Ann. Intern. Med*. 2022; 175(8):1143-1153.
8. Viana MdB, Aquino PEAd, Estadella D, Ribeiro DA, Viana GSdB. *Cannabis sativa* and Cannabidiol: A Therapeutic Strategy for the Treatment of Neurodegenerative Diseases? *Med. Cannabis Cannabinoids*. 2022; 5(1):207-219.
9. Cooper SY, Akers AT, Journigan VB, Henderson BJ. Novel putative positive modulators of α 4 β 2 nAChRs potentiate nicotine reward-related behavior. *Molecules*. 2021; 26(16):4793.
10. Wei T-T, Chandy M, Nishiga M, Zhang A, Kumar KK, Thomas D, Manhas A, Rhee S, Justesen JM, Chen IY. Cannabinoid receptor 1 antagonist genistein attenuates marijuana-induced vascular inflammation. *Cell*. 2022; 185(10):1676-1693.
11. Carstens E, Carstens MI. Sensory effects of nicotine and tobacco. *Nicotine Tob. Res*. 2022; 24(3):306-315.
12. Hoch E, Bonnet U, Thomasius R, Ganzer F, Havemann-Reinecke U, Preuss UW. Risks associated with the non-medical use of cannabis. *Dtsch. Ärztebl. Int*. 2015; 112(16):271.
13. Mura P, Udermer M, Brunet B. Cannabis: similarities and differences with tobacco. *Rev. Mal. Respir*. 2020; 37(6):479-447.
14. Kitchen C, Kabba JA, Fang Y. Status and impacts of recreational and medicinal cannabis policies in Africa: A systematic review and thematic analysis of published and "Gray" literature. *Cannabis Cannabinoid Res*. 2022; 7(3):239-261.
15. Otu SE. The "War on drugs" in Nigeria: How effective and beneficial is it in dealing with the problem? *Afr. J. Drug Alcohol Stud*. 2013; 12(2):119-135
16. Bridge J, Loglo M-G. Drug laws in West Africa: A review and summary. *Int. Drug Policy Consortium West Afr. Comm. Drugs*. 2017.
17. Oladepo O, Oluwasanu M, Abiona O. Analysis of tobacco control policies in Nigeria: historical development and application of multi-sectoral action. *BMC Public Health*. 2018; 18(1):1-12.
18. Chung EY, Cha HJ, Min HK, Yun J. Pharmacology and adverse effects of new psychoactive substances: synthetic cannabinoid receptor agonists. *Arch. Pharm. Res*. 2021; 44:402-413.
19. World Health Organization. WHO report on the global tobacco epidemic, 2021: addressing new and emerging products. *World Health Organ*. 2021.
20. Raies AB, Bajic VB. *In silico* toxicology: computational methods for the prediction of chemical toxicity. *Wiley Interdiscip. Rev. Comput. Mol. Sci*. 2016; 6(2):147-172.
21. Shaker B, Ahmad S, Lee J, Jung C, Na D. *In silico* methods and tools for drug discovery. *Comput. Biol. Med*. 2021; 137:104851.
22. Santos LH, Ferreira RS, Caffarena ER. Integrating molecular docking and molecular dynamics simulations. *Docking Screens Drug Discov*. 2019; 13-34.
23. Kar S, Leszczynski J. Open access *in silico* tools to predict the ADMET profiling of drug candidates. *Expert Opin. Drug Discov*. 2020; 15(12):1473-1487.
24. Singh S, Singh DB, Gautam B, Singh A, Yadav N. Pharmacokinetics and pharmacodynamics analysis of drug candidates. *Bioinformatics: Elsevier*; 2022. 305-316 p.
25. Rose PW, Prlić A, Altunkaya A, Bi C, Bradley AR, Christie CH, Costanzo LD, Duarte JM, Dutta S, Feng Z. The RCSB protein data bank: integrative view of protein, gene and 3D structural information. *Nucleic Acids Res*. 2016; gkw1000.
26. Tian W, Chen C, Lei X, Zhao J, Liang J. CASTp 3.0: computed atlas of surface topography of proteins. *Nucleic Acids Res*. 2018; 46(W1):W363-W367
27. Wang J, Wang W, Kollman PA, Case DA. Automatic atom type and bond type perception in molecular mechanical calculations. *J. Mol. Graph. Model*. 2006; 25(2):247-260.
28. Kim S, Thiessen PA, Bolton EE, Chen J, Fu G, Gindulyte A, Han L, He J, He S, Shoemaker BA. PubChem substance

- and compound databases. *Nucleic Acids Res.* 2016; 44(D1):D1202-D1213.
29. Borquaye LS, Gasu EN, Ampomah GB, Kyei LK, Amarah MA, Mensah CN, Nartey D, Commodore M, Adomako AK, Acheampong P. Alkaloids from *Cryptolepis sanguinolenta* as potential inhibitors of SARS-CoV-2 viral proteins: An *in silico* study. *Biomed Res. Int.* 2020; 2020(1):5324560.
 30. Trott O, Olson AJ. AutoDock Vina: improving the speed and accuracy of docking with a new scoring function, efficient optimization, and multithreading. *J. Comput. Chem.* 2010; 31(2):455-461.
 31. Kutzner C, Knip C, Cherian A, Nordstrom L, Grubmüller H, de Groot BL, Gapsys V. GROMACS in the cloud: A global supercomputer to speed up alchemical drug design. *J. Chem. Inf. Model.* 2022; 62(7):1691-1711.
 32. Mark P, Nilsson L. Structure and dynamics of the TIP3P, SPC, and SPC/E water models at 298 K. *J. Phys. Chem. A.* 2001; 105(43):9954-9960.
 33. Vanommeslaeghe K, Hatcher E, Acharya C, Kundu S, Zhong S, Shim J, Darian E, Guvench O, Lopes P, Vorobyov I. CHARMM general force field: A force field for drug-like molecules compatible with the CHARMM all-atom additive biological force fields. *J. Comput. Chem.* 2010; 31(4):671-690.
 34. Hanwell MD, Curtis DE, Lonie DC, Vandermeersch T, Zurek E, Hutchison GR. Avogadro: an advanced semantic chemical editor, visualization, and analysis platform. *J. Cheminform.* 2012; 4(1):17.
 35. Berendsen HJ, Postma Jv, Van Gunsteren WF, DiNola A, Haak JR. Molecular dynamics with coupling to an external bath. *J. Chem. Phys.* 1984; 81(8):3684-3690.
 36. Ogunlana AT, Boyenle ID, Ojo TO, Quadri BO, Elegbeleye OE, Ogbonna HN, Ayoola SO, Badmus IO, Manica AK, Joshua KI. Structure-based computational design of novel covalent binders for the treatment of sickle cell disease. *J. Mol. Graph. Model.* 2023; 124:108549.
 37. Daina A, Michielin O, Zoete V. SwissADME: a free web tool to evaluate pharmacokinetics, drug-likeness and medicinal chemistry friendliness of small molecules. *Sci. Rep.* 2017; 7(1):42717.
 38. Banerjee P, Eckert AO, Schrey AK, Preissner R. ProTox-II: a webserver for the prediction of toxicity of chemicals. *Nucleic Acids Res.* 2018; 46(W1).
 39. Adelusi TI, Oyedele A-QK, Boyenle ID, Ogunlana AT, Adeyemi RO, Ukachi CD, Idris MO, Olaoba OT, Adedotun IO, Kolawole OE. Molecular modeling in drug discovery. *Inform. Med. Unlocked.* 2022; 29:100880.
 40. Salo-Ahen OM, Alanko I, Bhadane R, Bonvin AM, Honorato RV, Hossain S, Juffer AH, Kabedev A, Lahtela-Kakkonen M, Larsen AS. Molecular dynamics simulations in drug discovery and pharmaceutical development. *Processes.* 2020; 9(1):71.
 41. Shagal M, Modibbo U, Liman A. Pharmacological justification for the ethnomedical use of *Datura stramonium* stem-bark extract in treatment of diseases caused by some pathogenic bacteria. *Int Res Pharm Pharmacol.* 2012; 2(1):16-19.
 42. Oseni O, Olarinoye C, Amoo I. Studies on chemical compositions and functional properties of thorn apple (*Datura stramonium* L) Solanaceae. *Afr J Food Sci.* 2011; 5(2):40-44.
 43. Umamaheswari M, Aji C, Asokkumar K, Sivashanmugam T, Subhadradevi V, Jagannath P, Madeswaran A. Docking studies: *In silico* aldose reductase inhibitory activity of commercially available flavonoids. *Bangladesh J Pharmacol.* 2012; 7(2):108-113.
 44. Sharma A, Sharma R, Sharma M, Kumar M, Barbhai MD, Lorenzo JM, Sharma S, Samota MK, Atanassova M, Caruso G. *Carica papaya* L. leaves: Deciphering its antioxidant bioactives, biological activities, innovative products, and safety aspects. *Oxid Med Cell Longev.* 2022; 2022(1):5594781.
 45. Wadekar AB, Nimbawar MG, Panchale WA, Gudalwar BR, Manwar JV, Bakal RL. Morphology, phytochemistry and pharmacological aspects of *Carica papaya*, a review. *GSC Biol Pharm Sci.* 2021; 14(3):234-248.
 46. Julianti T, Oufir M, Hamburger M. Quantification of the antiparasmodial alkaloid carpine in papaya (*Carica papaya*) leaves. *Planta Med.* 2014; 80(13):1138-1142.
 47. Gorane A, Naik A, Nikam T, Tripathi T, Ade A. GCMS analysis of phytochemicals of *C. papaya* variety red lady. *J Pharmacogn Phytochem.* 2018; 7(2):553-555.
 48. Oyewole AL, Owoyele BV. Neurobehavioural effects of exposure of Wistar rats to smoke from traditional *Carica papaya* (pawpaw) leaves. *CellMed.* 2012; 2(4):36.1-4.
 49. Afzan A, Abdullah NR, Halim SZ, Rashid BA, Semail RHR, Abdullah N, Jantan I, Muhammad H, Ismail Z. Repeated dose 28-days oral toxicity study of *Carica papaya* L. leaf extract in Sprague Dawley rats. *Molecules.* 2012; 17(4):4326-4342.
 50. Ovando-Martínez M, González-Aguilar GA. Papaya. Nutritional composition and antioxidant properties of fruits and vegetables: Elsevier; 2020. 499-513 p.
 51. Saran P, Choudhary R. Drug bioavailability and traditional medicaments of commercially available papaya: A review. *Afr J Agric Res.* 2013; 8(25):3216-3223.
 52. Hiraga Y, Ara T, Sato N, Akimoto N, Sugiyama K, Suzuki H, Kera K. Metabolic analysis of unripe papaya (*Carica papaya* L.) to promote its utilization as a functional food. *Biosci Biotechnol Biochem.* 2021; 85(5):1194-1204.
 53. Lentz TL, Chaturvedi V, Conti-Fine BM. Amino acids within residues 181–200 of the nicotinic acetylcholine receptor $\alpha 1$ subunit involved in nicotine binding. *Biochem Pharmacol.* 1998; 55(3):341-347.
 54. Delgado-Vélez M, Quesada O, Villalobos-Santos JC, Maldonado-Hernández R, Asmar-Rovira G, Stevens RC, Lasalde-Dominicci JA. Pursuing high-resolution structures of nicotinic acetylcholine receptors: lessons learned from five decades. *Molecules.* 2021; 26(19):5753.
 55. Xiu X, Puskar NL, Shanata JA, Lester HA, Dougherty DA. Nicotine binding to brain receptors requires a strong cation- π interaction. *Nature.* 2009; 458(7237):534-537.
 56. Naha A, Banerjee S, Debroy R, Basu S, Ashok G, Priyamvada P, Kumar H, Preethi A, Singh H, Anbarasu A. Network metrics, structural dynamics and density functional theory calculations identified a novel Ursodeoxycholic Acid derivative against therapeutic target Parkin for Parkinson's disease. *Comput Struct Biotechnol J.* 2022; 20:4271-4287.
 57. Pansar T, Poso A. Binding affinity via docking: fact and fiction. *Molecules.* 2018; 23(8):1899.
 58. Nogueira MS, Koch O. The development of target-specific machine learning models as scoring functions for docking-based target prediction. *J Chem Inf Model.* 2019; 59(3):1238-1252.
 59. Guan L, Yang H, Cai Y, Sun L, Di P, Li W, Liu G, Tang Y. ADMET-score—a comprehensive scoring function for evaluation of chemical drug-likeness. *MedChemComm.* 2019; 10(1):148-157.
 60. Chen X, Li H, Tian L, Li Q, Luo J, Zhang Y. Analysis of the physicochemical properties of acaricides based on Lipinski's rule of five. *J Comput Biol.* 2020; 27(9):1397-1406.
 61. Ibrahim ZYu, Uzairu A, Shallangwa G, Abechi S. Molecular docking studies, drug-likeness and *in-silico* ADMET prediction of some novel β -Amino alcohol grafted 1, 4, 5-trisubstituted 1, 2, 3-triazoles derivatives as elevators of p53 protein levels. *Sci Afr.* 2020; 10:e00570
 62. Hai, NTT, Huong, DTQ, Hoang, NV, Bui, TQ, Quy, PT, Phu, NV, Chau, ND, Huy, TQ, Hue, DT, Nhung, NTA.

Antibacterial Potentials of *Blumea balsamifera*. Essential Oil Against *Streptococcus pyogenes* and *Streptococcus pneumoniae*: *In Vitro* and *In Silico* Screening. Trop J Nat Prod Res. 2024; 8(6): 7590 –7602.

63. Al Dhaheri Y, Wali AF, Akbar I, Rasool S, Razmpoor M, Jabnoun S, Rashid S. *Nigella sativa*, a cure for every disease: Phytochemistry, biological activities, and clinical trials. *Black Seeds (Nigella Sativa)*: Elsevier; 2022. 63-90 p.
64. Price G, Patel DA. Drug bioavailability. 2020. PMID: 32496732.
65. Poongavanam V, Haider N, Ecker GF. Fingerprint-based *in silico* models for the prediction of P-glycoprotein substrates and inhibitors. *Bioorg Med Chem*. 2012; 20(18):5388-5395.
66. Shityakov S, Förster C. *In silico* structure-based screening of versatile P-glycoprotein inhibitors using polynomial empirical scoring functions. *Adv Appl Bioinform Chem*. 2014; 7:1.
67. Rahayu S, Widyarti S, Soewondo A, Prasetyaningrum DI, Umarudin U. A Computational Insights of *Ocimum basilicum* Flavonoid and Essential Oils Interaction in the Targeting Keap1/SIRT1/NFκB Signaling Pathway. Trop J Nat Prod Res. 2024; 8(2):6182-6191.